Estimating turbogenerator foundation parameters

M Smart, **M I Friswell**, **A W Lees** and **U Prells**
Department of Mechanical Engineering, University of Wales Swansea, Wales

Abstract: Turbogenerators in power stations are often placed on foundation structures that are flexible over the running range of the machine and can therefore contribute to its dynamics. Established methods of obtaining structural models for these foundations, such as the finite element method or modal testing, have proved unsuccessful because of complexity or cost. Another method of foundation system identification, using the unbalance excitation applied by the rotor itself during maintenance run-downs, has previously been proposed but has not yet been experimentally verified. In this paper the necessary theory is developed and certain issues critical to the success of the estimation are examined. The method is tested in both simulation and experiment using a two-bearing rotor rig and good fits between model and measurement are obtained. The predictive capacity of the estimated models when the system is excited with a different unbalance is not as good, and it is surmised that this may be due among other things to inaccurate bearing models.

Keywords: system identification, rotating machinery, modelling, vibration

NOTATION

$\mathbf{C}_B$, $\mathbf{C}_F$, $\mathbf{C}_R$	damping matrices for bearing, foundation and rotor
$\mathbf{D}_B$, $\mathbf{D}_R$	dynamic stiffness matrices for bearing and rotor
$\bar{\mathbf{D}}_F$	condensed dynamic stiffness matrix for foundation
$\boldsymbol{f}_F$	foundation force vector
$\boldsymbol{f}_u$	unbalanced force vector
$\mathbf{G}_R$	gyroscopic matrix for rotor
$\boldsymbol{h}$	product of inverse dynamic stiffness matrix and forces
$\mathbf{I}$	identity matrix
$\mathrm{j}\omega$	complex frequency
J_i, J_o	cost functions
$\bar{k}_{F,ij}$, $\bar{c}_{F,ij}$, $\bar{m}_{F,ij}$	ijth elements of $\bar{\mathbf{K}}_F$, $\bar{\mathbf{C}}_F$ and $\bar{\mathbf{M}}_F$
$\mathbf{K}_B$, $\mathbf{K}_F$, $\mathbf{K}_R$	stiffness matrices for bearing, foundation and rotor
$\bar{\mathbf{K}}_F$, $\bar{\mathbf{C}}_F$, $\bar{\mathbf{M}}_F$	condensed foundation stiffness, damping and mass matrices
$\mathbf{M}_F$, $\mathbf{M}_R$	mass matrices for foundation and rotor
n	measured DOF of foundation
p	total number of frequency points
$\mathbf{P}$	manipulation matrix
$\boldsymbol{q}$	vector of force elements at all frequencies
$\mathbf{R}_0$, $\mathbf{R}_1$, $\mathbf{R}_2$	matrices containing displacements
$\mathbf{T}$	transformation matrix
$\mathbf{V}$	matrix containing displacements at all frequencies
$\mathbf{V}_c$	matrix containing constrained displacements at all frequencies
$\mathbf{W}$	weighting matrix
x, y	foundation translational DOF
$\boldsymbol{x}_R$, $\boldsymbol{x}_F$	displacement vectors for rotor and foundation
$\boldsymbol{\alpha}$	vector of parameters
$\boldsymbol{\alpha}_c$	vector of constrained parameters
$\boldsymbol{\varepsilon}_i$, $\boldsymbol{\varepsilon}_o$	input and output error function vectors
$\boldsymbol{\theta}_x$, $\boldsymbol{\theta}_y$	foundation rotational DOF
ω_s, ω_f	starting, finishing frequencies
Ω	rotor running speed

The MS was received on 5 September 1997 and was accepted for publication on 28 April 1998.

1 INTRODUCTION

Turbogenerators in modern power stations are normally built on flexible steel foundations which may have many natural frequencies over the running range of the machine. They can therefore have a significant effect on the dynamics of the machine during run-up and run-down. Condition monitoring techniques, which use measurements of vibration to detect and possibly locate faults, often require good dynamic models of the turbogenerator.

The modelling of the dynamics of the rotors in turbogenerators is well established, with designers confident enough of their predictions to operate well into the post-critical range. However, the influence of the foundation structure on the machine's dynamic response is not so well understood. Attempts have been made to model the turbogenerator foundations using the finite element method, but the complexity of the foundations and the fact that they often differ substantially from the original drawings have made the technique generally unsuccessful [**1**].

Experimental modal analysis is another way of obtaining the foundation dynamic response [**2**], but in order to achieve this the rotor must be removed from the foundation while all casings remain in place. The excessive cost in station downtime normally makes this prohibitively expensive. However, in order to satisfy maintenance requirements, turbogenerators are normally run down from operating speed to rest at regular intervals. This procedure applies a frequency dependent force to the foundation which may be estimated, and since the response at the bearing pedestals is measured for condition monitoring purposes an input–output relation for the foundation may be obtained.

Lees [**3**] developed a method that calculated the forces applied to the foundation at the bearings and used these calculated forces together with the measured responses to derive the foundation parameters using least-squares estimation. The method required models for the rotor and bearing dynamic stiffness, as well as prior knowledge of the state of unbalance of the machine. The measurements were taken at the bearing pedestals. He demonstrated the technique using a very simple two-bearing model with speed independent characteristics. Vania [**4**] followed a similar approach but used Kalman filters to estimate the parameters.

Feng and Hahn [**5**] used a similar approach which made use of shaft displacement measurements and thereby reduced the dependence on a priori models of the rotor and bearings. However, many turbines in British power stations are not equipped with proximitors and so this extra information is not often available. Again, this method was tested in simulation but no experimental data was provided. Zanetta [**6**] did not assume that adequate models of the bearings existed, but rather estimated a model which combined bearings and foundation.

The organization of the paper is as follows. Firstly the theory presented in [**3**] is expanded, showing how forces on the foundation are estimated using models of the rotor and bearings. These forces and the measured foundation displacements are used to set up an input–output equation for the foundation. From this equation cost functions based on input and output residuals are set up and minimized, leading to linear and non-linear least-squares estimates of the foundation parameters. Some tests for the quality of the estimated model are proposed and the effect of errors on the estimates are considered. Finally, the theory is tested on a two-bearing rotor rig, firstly in simulation using a foundation finite element model and then in experiment.

2 THEORY

Figure 1 is an abstract representation of a turbogenerator, whereby a rotor is connected to a flexible foundation via oil-film journal bearings. The foundation estimation algorithm proceeds in two steps:

1. Known models of the rotor and bearing are used to estimate the forces acting on the foundation corresponding to a given set of foundation measurements.
2. These predicted forces are then taken together with the measurements and used to estimate dynamic stiffness parameters for the foundation.

2.1 Force estimation

The dynamic stiffness equation of the entire structure is

$$\begin{bmatrix} \mathbf{D}_{R,ii} & \mathbf{D}_{R,ib} & \mathbf{0} \\ \mathbf{D}_{R,bi} & \mathbf{D}_{R,bb}+\mathbf{D}_B & -\mathbf{D}_B \\ \mathbf{0} & -\mathbf{D}_B & \mathbf{D}_B+\bar{\mathbf{D}}_F \end{bmatrix} \begin{pmatrix} \boldsymbol{x}_{R,i} \\ \boldsymbol{x}_{R,b} \\ \boldsymbol{x}_{F,b} \end{pmatrix} = \begin{pmatrix} \boldsymbol{f}_u \\ \boldsymbol{0} \\ \boldsymbol{0} \end{pmatrix} \tag{1}$$

where subscripts i and b refer to partitioning into internal and bearing (connection) DOF respectively. This may be used to derive an expression for the forces acting on the foundation at the bearings

$$\boldsymbol{f}_{F,b} = \boldsymbol{D}_B[(\mathbf{P}^{-1}\mathbf{D}_B - \mathbf{I})\boldsymbol{x}_{F,b} - \mathbf{P}^{-1}\mathbf{D}_{R,bi}\mathbf{D}_{R,ii}^{-1}\boldsymbol{f}_u] \tag{2}$$

where $\mathbf{P} = \mathbf{D}_{R,bb} + \mathbf{D}_B - \mathbf{D}_{R,bi}\mathbf{D}_{R,ii}^{-1}\mathbf{D}_{R,ib}$.

It is assumed that models for the rotor and bearing exist and that the unbalance is known. Therefore $\mathbf{D}_R$,

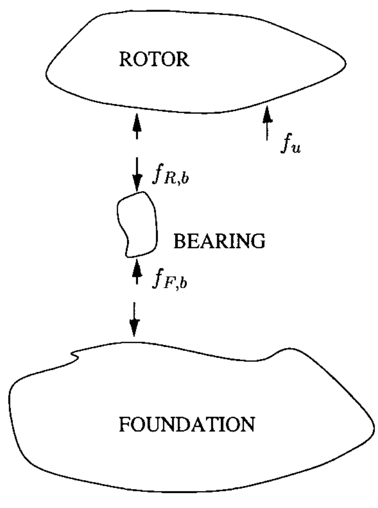

Fig. 1 Rotor on bearings and foundation

$\mathbf{D}_B$ and $\boldsymbol{f}_u$ are all available and the foundation forces may be estimated based on the measured response of the foundation.

2.2 Foundation identification

Once the foundation forces have been estimated, a suitable foundation model that matches the measured responses to the estimated forces must be found. The reduced dynamic stiffness matrix for the foundation relating forces to displacements is

$$\bar{\mathbf{D}}_F \boldsymbol{x}_{F,b} = \boldsymbol{f}_{F,b} \tag{3}$$

The essence of the identification problem is finding a suitable $\bar{\mathbf{D}}_F$. There are a number of stages to this process [**7**, **8**]:

(a) model selection and parameterization,
(b) parameter estimation,
(c) model verification,
(d) model validation.

2.3 Model selection and parameterization

The first step involves the selection of a set of models out of the infinite number of possible models, which guarantees a 'sensible' identification problem. A widely used method for modelling linear, time-invariant structure in the frequency domain is the frequency filter [**9**–**11**], whereby equation (3) is represented as

$$[\bar{\mathbf{K}}_F + j\omega \bar{\mathbf{C}}_F + (j\omega)^2 \bar{\mathbf{M}}_F] \boldsymbol{x}_{F,b} = \boldsymbol{f}_{F,b} \tag{4}$$

These matrices will contain as many modes as the measured foundation DOF, which may be different from the number of modes present in the data. If there are more modes than DOF, the frequency range may be split up into intervals for which individual estimates are found. If there are less modes than DOF, then in theory rank deficient matrices will result, although in practice noise on the data will generate spurious modes, which must be identified and rejected [**12**–**14**]. The elements of $\bar{\mathbf{M}}_F$, $\bar{\mathbf{C}}_F$ and $\bar{\mathbf{K}}_F$ are the parameters which must be estimated.

2.4 Parameter estimation

Once the model has been selected and parameterized, a set of parameters that minimizes the error between model and system must be found. This is normally accomplished by defining residuals, which represent the difference between measurements and estimates. These residuals depend on the parameters that must be found, so cost functions of the residuals are set up and minimized to generate parameter estimates.

Two commonly used residuals are input error residuals and output error residuals. Cost functions of these errors are then minimized to find the relevant parameters:

$$\min J_i = \int_{\omega_s}^{\omega_f} \boldsymbol{\varepsilon}_i^H \mathbf{W} \boldsymbol{\varepsilon}_i \, d\omega \qquad \boldsymbol{\varepsilon}_i = \bar{\mathbf{D}}_F \boldsymbol{x}_{F,b} - \boldsymbol{f}_{F,b} \tag{5a}$$

$$\min J_o = \int_{\omega_s}^{\omega_f} \boldsymbol{\varepsilon}_o^H \mathbf{W} \boldsymbol{\varepsilon}_o \, d\omega \qquad \boldsymbol{\varepsilon}_o = \boldsymbol{x}_{F,b} - \bar{\mathbf{D}}_F^{-1} \boldsymbol{f}_{F,b} \tag{5b}$$

It is well known (see, for example, references [**11**] and [**15**]) that the estimation problem defined by equation (5a) is linear in parameters, while equation (5b) is non-linear in parameters. The linear problem is easily solved by the least squares method. In the case of noisy data the estimates have a bias, which may be reduced by an instrumental variable method [**11**, **16**, **17**]. The non-linear estimation process, on the other hand, is more robust with respect to noise but must be solved using an iterative technique, with the usual problems of convergence and the need for a good starting solution.

2.4.1 Linear input error parameter estimation

If there are n measured DOF in the foundation, equation (4) may be rewritten as

$$[\mathbf{R}_0 \;\; \mathbf{R}_1 \;\; \mathbf{R}_2](\boldsymbol{\alpha}) = (\boldsymbol{f}_{F,b}) \tag{6}$$

where

$$\mathbf{R}_k = (j\omega)^k \begin{bmatrix} \boldsymbol{x}_{F,b}^T & \boldsymbol{0} & \cdots & \boldsymbol{0} \\ \boldsymbol{0} & \boldsymbol{x}_{F,b}^T & & \boldsymbol{0} \\ \vdots & \vdots & \ddots & \vdots \\ \boldsymbol{0} & \cdots & \boldsymbol{0} & \boldsymbol{x}_{F,b} \end{bmatrix} \tag{7}$$

and the vector of parameters $\boldsymbol{\alpha}$ is

$$\begin{aligned} \boldsymbol{\alpha}^T = (&\bar{k}_{F,11} \; \bar{k}_{F,12} \cdots \bar{k}_{F,nn} \cdots \\ &\bar{c}_{F,11} \; \bar{c}_{F,12} \cdots \bar{c}_{F,nn} \cdots \\ &\bar{m}_{F,11} \; \bar{m}_{F,12} \cdots \bar{m}_{F,nn}) \end{aligned} \tag{8}$$

Equation (6) may be repeated for all frequency points:

$$\mathbf{V}\boldsymbol{\alpha} = \boldsymbol{q} \tag{9}$$

$$\mathbf{V} = \begin{bmatrix} \mathbf{R}_0(j\omega_1) & \mathbf{R}_1(j\omega_1) & \mathbf{R}_2(j\omega_1) \\ \mathbf{R}_0(j\omega_2) & \mathbf{R}_1(j\omega_2) & \mathbf{R}_2(j\omega_2) \\ \vdots & \vdots & \vdots \\ \mathbf{R}_0(j\omega_p) & \mathbf{R}_1(j\omega_p) & \mathbf{R}_2(j\omega_p) \end{bmatrix} \qquad \boldsymbol{q} = \begin{pmatrix} \boldsymbol{f}_{F,b}(j\omega_1) \\ \boldsymbol{f}_{F,b}(j\omega_2) \\ \vdots \\ \boldsymbol{f}_{F,b}(j\omega_p) \end{pmatrix} \tag{10}$$

2.4.2 *Constraints and scaling*

The above formulation assumes that all values in the dynamic stiffness matrix are independent. In practice of course this is not so—real structures normally obey Maxwell's reciprocity theorem and are therefore symmetrical. This can be taken into account by means of a transformation matrix, $\mathbf{T}$:

$$\mathbf{T}\boldsymbol{\alpha}_c = \boldsymbol{\alpha} \tag{11}$$

where $\boldsymbol{\alpha}_c$ are the constrained parameters. Then

$$\mathbf{V}_c\boldsymbol{\alpha}_c = \boldsymbol{q} \tag{12}$$

where $\mathbf{V}_c = \mathbf{VT}$.

Provided that the number of equations is greater than the total number of parameters, equation (12) will be overdetermined and may be solved using any least-squares algorithm. This will minimize the input error defined in equation (5a).

Two types of scaling may be applied to the least-squares problem [**18**]. The first is row scaling, to take into account the fact that the forces increase with ω^2, and therefore the higher-frequency data will carry more weight in the equations, even though they are further away from the region dominated by the foundation dynamics. The rows of equation (12) were therefore scaled by the frequency vector.

Column scaling is necessary because of the different magnitudes of the elements of the $\bar{\mathbf{M}}_F$, $\bar{\mathbf{C}}_F$ and $\bar{\mathbf{K}}_F$ matrices, and the scaling factor used here was the mean value of ω.

2.4.3 *Non-linear, output error parameter estimation*

Referring to equation (4), let $\boldsymbol{h}$ be the product of the inverse dynamic stiffness matrix and the forces:

$$\boldsymbol{h}(\mathrm{j}\omega, \boldsymbol{\alpha}) = [\bar{\mathbf{K}}_F + (\mathrm{j}\omega)\bar{\mathbf{C}}_F + (\mathrm{j}\omega)^2\bar{\mathbf{M}}_F]^{-1}\boldsymbol{f}_{F,b} \tag{13}$$

where $\boldsymbol{h}$ depends on both the frequency and the parameters that must be estimated. Then the output error from equation (5b) is

$$\boldsymbol{\varepsilon}_o = \boldsymbol{x}_{F,b} - \boldsymbol{h} \tag{14}$$

This must be minimized over all frequencies to give the required parameters. Since $\boldsymbol{h}$ depends on the parameters as well as the frequency, an iterative routine is required. For this research a Levenberg–Marquardt algorithm was used for the non-linear estimation procedure, which is efficient and has reasonable convergence properties [**19**, **20**]. The parameter estimates from the linear least-squares routine were used as starting estimates. The application of constraints and scaling of the parameters may be done as for the linear least-squares case.

2.5 Model verification

When the estimation procedure is complete, a first check of the adequacy of the model so obtained is by examining the relative magnitudes of the residuals (input error and output error in the present case) to determine the quality of fit. This can give an indication as to the quality of the estimated model.

2.6 Model validation

The next test of the estimated model is subjecting it and the real system to a different excitation and comparing the residuals between system and model. This is a more rigorous check than simply checking the original residuals. The final test is obtaining independent estimates of the parameters through a different testing method.

2.7 Errors in the model

Smart *et al.* [**16**] considered the effect of various errors on the estimation routine. Firstly, errors may arise when estimating the foundation forces [equation (2)] owing to erroneous bearing models, rotor models or unbalance estimation, as well as to noise in the measurements. Secondly, errors can arise during the parameter estimation process.

Since the rotors are normally symmetric structures manufactured to tight tolerances from materials whose properties are well characterized, it is reasonable to assume that models of these rotors will be accurate. As will be seen in the section on experimentation, the frequencies generated from rotor models compared very well with those obtained from free–free impact testing.

The state of unbalance may in theory be established from a balancing run. If two successive run-downs are performed, one due to the unknown system unbalance and one with known balance weights attached, then provided the system is linear the response measurements may be vectorially subtracted to give the response due to the known balance weights alone. This is the basis for the balancing of industrial machines, so significant errors are not expected in the assumed unbalance distribution.

The stiffness and damping matrices for the journal bearings are estimated using short bearing theory [**21**]. Experimental tests on journal bearings have shown reasonable agreement between theoretical and measured values [**22**]. However, good estimates are dependent on an accurate knowledge of the static force being applied to the bearings, which is not always easy to calculate. Therefore it must be assumed that the stiffness and damping estimates for the bearings can introduce significant errors into the foundation parameter estimation.

Finally, noise on the measurements will affect both input and output sides of the least-squares and non-linear least-squares equations. This can be, for example, electrical or digitization noise (which are typically

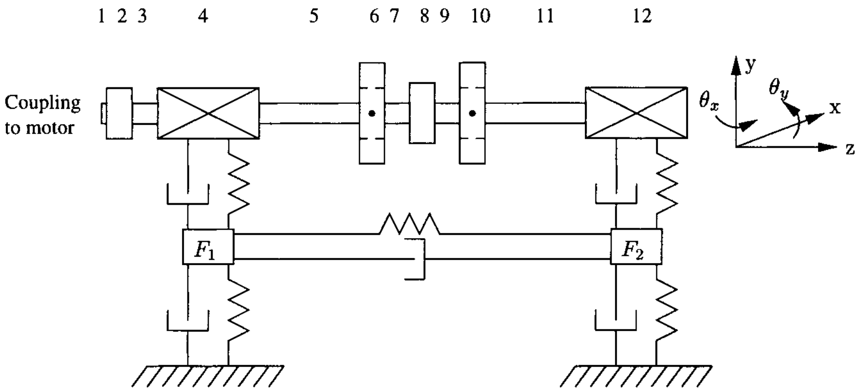

Fig. 2 Diagram of two-bearing rotor rig

regarded as being normally distributed) or noise arising from the order tracking routines.

3 SIMULATION

3.1 Description of rig

The foundation model estimation method was tested on a small rig located at Aston University, Birmingham. This consists of a steel shaft approximately 1.1 m long with a nominal diameter of 38 mm and two shrink-fitted balancing discs. The shaft is supported at either end by a journal bearing of 100 mm diameter with a length–diameter ratio of 0.3 and a radial clearance of 125 μm. The bearings contain oil with a viscosity of 0.009 N s/m^2 and are supported on flexible pedestals, with the pedestals bolted on to a large lathe bed. The rig is powered by a 3.7 kW d.c. motor, attached via a belt to a driving pulley which is in turn attached via a flexible coupling to the main rotor shaft. The speed is measured using an optical shaft encoder which provides a 5 V pulse per revolution.

A schematic of the rig is shown in Fig. 2. Dimensions of each station and material properties are given in Table 1. Table 2 shows the different unbalance configurations used to excite the rotor. A finite element model was created for the rotor with 23 two-noded Euler beam elements, each with two translational and two rotational DOF. Short bearing theory was used to obtain values for the bearing stiffness and damping [**21**], assuming a mean static force of 300 N. The entire rig was assumed to be constrained along the axial direction of the rotor.

The pedestals themselves consist of two rectangular steel plates measuring 600 × 150 mm which have two channels cut into them and which are supported on knife edges. The vertical stiffness arises from the hinge effect of the channels, while the horizontal stiffness is as a result of the shaft centre tilting under an applied load.

For the purposes of simulation, the following mass, damping and stiffness matrices were used for the foundation, assuming that the displacement vector of the foundations is ordered as

$$\boldsymbol{x}_{\mathrm{F}}^{\mathrm{T}} = [x_1 \theta_{x1} y_1 \theta_{y1} x_2 \theta_{x2} y_2 \theta_{y2}]$$

where x and y are horizontal and vertical directions, and 1 and 2 refer to the foundations F_1 and F_2 in Fig. 2:

Table 1 Table of rotor rig physical properties

Station	Length (mm)	Diameter (mm)	E (GPa)	ρ (kg/m^3)
Shaft properties				
1	6.35	38.1	200	7850
2	25.4	77.57	200	7850
3	50.8	38.1	200	7850
4	203.2	100	200	7850
5	117.8	38.1	200	7850
6	50.8	116.8	200	7850
7	76.2	38.1	200	7850
8	76.2	109.7	200	7850
9	76.2	38.1	200	7850
10	50.8	102.9	200	7850
11	117.8	38.1	200	7850
12	203.2	100	200	7850
Balancing discs				
6	25.4	203.2		
10	25.4	203.2		

Table 2 Unbalance configurations used to excite rotor

Unbalance configuration	Balance disc	Unbalance (kg/m)	Phase (deg lead)
1	1	0	0
	2	0	0
2	1	0.0013	75
	2	0.0013	−150
3	1	0.0013	−105
	2	0.0013	120

$$\mathbf{K}_F = \begin{bmatrix} 1.50 & -0.60 & -0.10 & 0 & -0.50 & 0 & 0 & 0 \\ & 2.50 & 0 & 0 & 0 & 0 & 0 & 0 \\ & & 0.55 & -0.30 & 0 & 0 & -0.50 & 0 \\ & & & 2.50 & 0 & 0 & 0 & 0 \\ & \text{SYM} & & & 1.60 & -0.62 & -0.12 & 0 \\ & & & & & 2.40 & 0 & 0 \\ & & & & & & 0.57 & -0.32 \\ & & & & & & -0.32 & 2.40 \end{bmatrix} \text{MN/m} \quad (15a)$$

$$\mathbf{C}_F = \text{diag}[150\ \ 150\ \ 150\ \ 150\ \ 150\ \ 150\ \ 150\ \ 150]\ \text{N s/m} \quad (15b)$$

$$\mathbf{M}_F = \text{diag}[50\ \ 200\ \ 50\ \ 200\ \ 52\ \ 210\ \ 52\ \ 210]\ \text{kg} \quad (15c)$$

These matrices were derived using results of a modal test performed on the foundation without the rotor in place. They were not intended to give an accurate representation of the foundation but rather a representative one, broadly reproducing the kind of behaviour which would be expected in practice.

3.2 Results and discussion

The estimation theory was then tested using the model just described. The finite element model was used to generate responses at the bearings for frequencies from 0 to 40 Hz with a spacing of 0.25 Hz. Although each bearing has four DOF, it is assumed that only the translational DOF are measured. These measured responses were corrupted by normally distributed random noise with zero mean and standard deviation of 1 per cent of the maximum response amplitude (applied to both real and imaginary parts of the response). At each frequency the bearing static forces were disturbed by noise drawn from a uniform distribution spanning an interval of 20 per cent of the force magnitude to introduce uncertainty into the bearing parameters. The second unbalance configuration of Table 2 was taken as excitation for the system.

The forces on the foundation were calculated using the noisy 'measured' data and erroneous bearing model, and these forces together with the noisy displacements were used to estimate the foundation parameters. The estimated foundation model was then used to calculate the foundation displacements. Although there are only four measured DOF, there are more than four foundation modes in the frequency range under consideration, so the frequency band was split up into parts and foundation models estimated for each part.

Once a foundation model was estimated, it had to be verified and validated. Verification is accomplished by examining the residuals defined in equations (5a) and (5b). These are most easily interpreted graphically. Figures 3 and 4 show the forces acting on the foundation for the simulation, as well as estimates from the linear

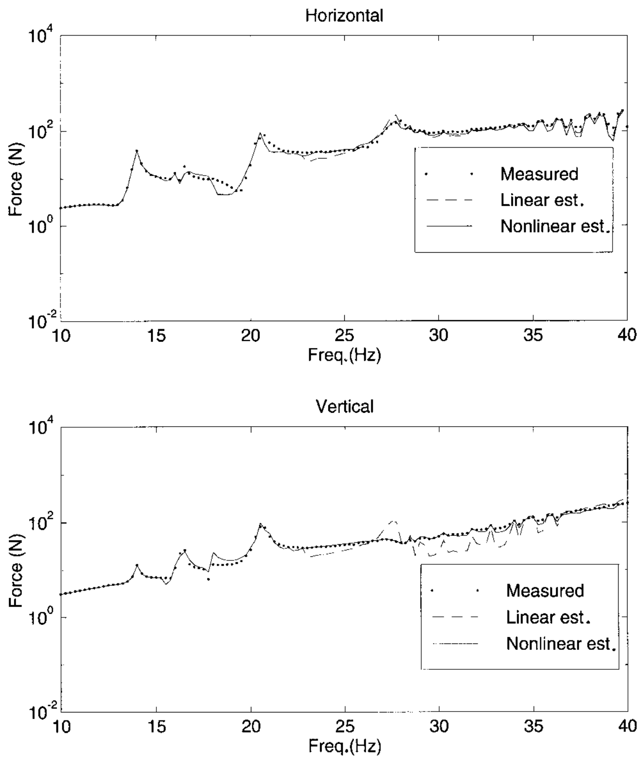

Fig. 3 Simulated and calculated forces for bearing 1

(input error) and non-linear (output error) foundation model estimates. The fit is good, although the linear estimate shows a spurious peak around 15 Hz. Figures 5 and 6 show the simulated responses at the foundation, as well as the estimates from the linear and non-linear least-squares foundation models. Again, the fit is good, with the displacements from the non-linear least-squares estimated model providing the best results.

Regarding model validation, Figs 7 to 10 show the forces and displacements when the model with estimated foundation is excited with a different unbalance configuration. In this case the results are not as good, especially for the linear least-squares estimates, but the nonlinear estimates do provide reasonable fit for the simulated results.

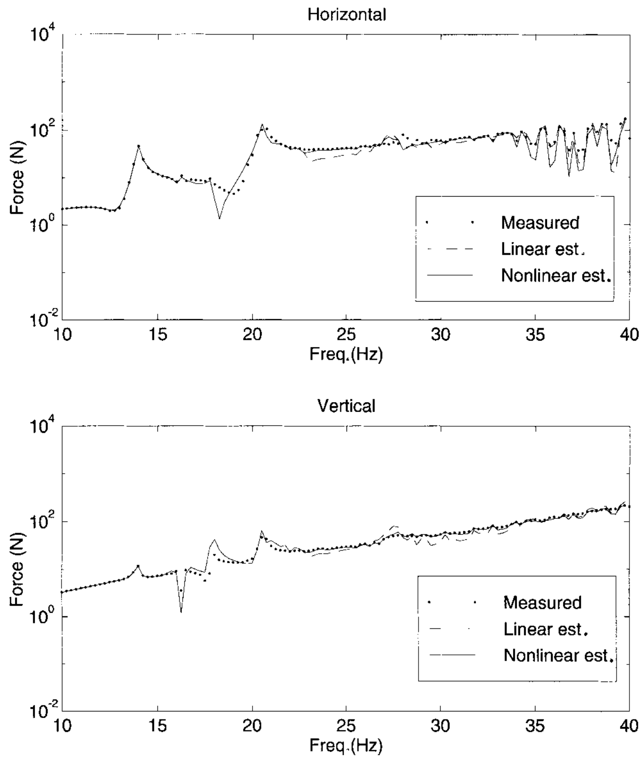

Fig. 4 Simulated and calculated forces for bearing 2

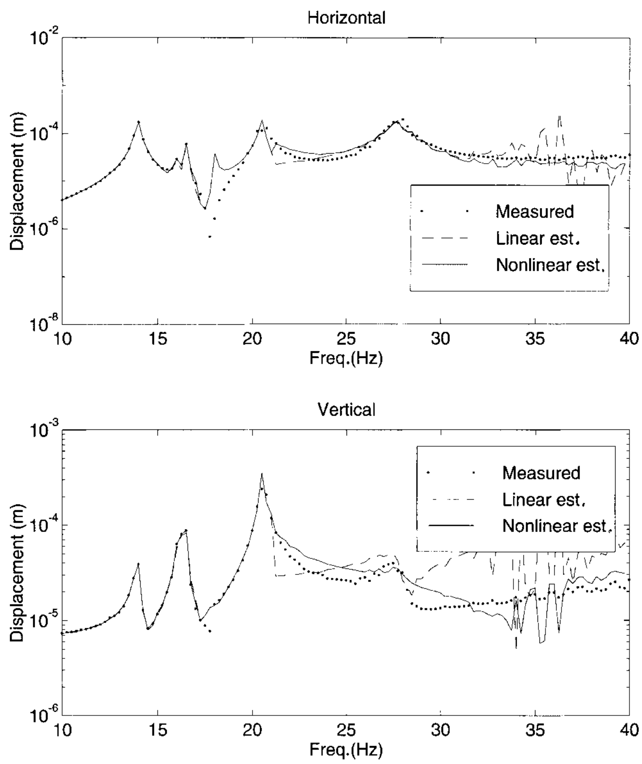

Fig. 5 Simulated and calculated displacements for bearing 1

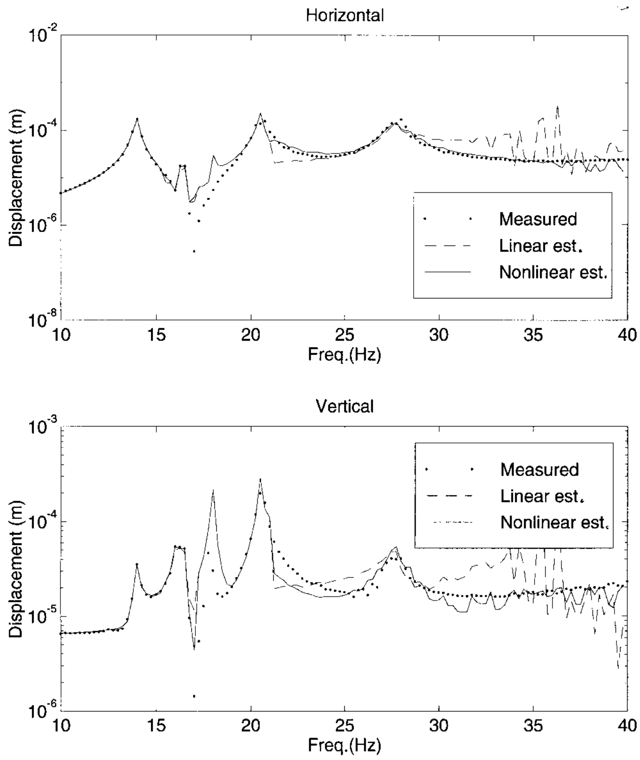

Fig. 6 Simulated and calculated displacements for bearing 2

The final test of the foundation model is comparing the estimated parameters to those obtained in an independent manner. For simulated results, the estimated parameters can be compared with those of the system used to obtain simulated results. The easiest way of doing this is through natural frequencies and damping factors. Table 3 shows the natural frequencies and damping factors of the foundation, both theory and estimates. There are four frequency ranges and four natural frequency estimates for each range, making a total of 16. However, any modes which were overdamped ($\zeta > 100\%$) or unstable ($\zeta < 0$) were rejected. This left eight frequencies for the model that was estimated using linear least squares, and 10 for the model that was estimated using non-linear least squares.

Table 3 Estimated foundation frequencies and damping factors for simulated example

Theory		Input error estimates		Output error estimates	
f (Hz)	ζ (%)	f (Hz)	ζ (%)	f (Hz)	ζ (%)
1.80	12.30	15.48	0.96	15.01	1.66
15.02	0.61	17.82	2.36	16.72	0.53
16.48	0.44	18.73	5.86	17.93	0.42
16.69	0.42	22.74	1.27	18.59	2.42
18.06	0.39	25.04	3.16	20.54	0.54
23.35	0.93	26.43	23.68	23.00	0.67
24.56	0.81	28.95	44.26	24.56	14.29
32.47	0.70	31.42	3.51	31.14	0.63
—	—	—	—	32.33	9.91
—	—	—	—	36.16	2.43

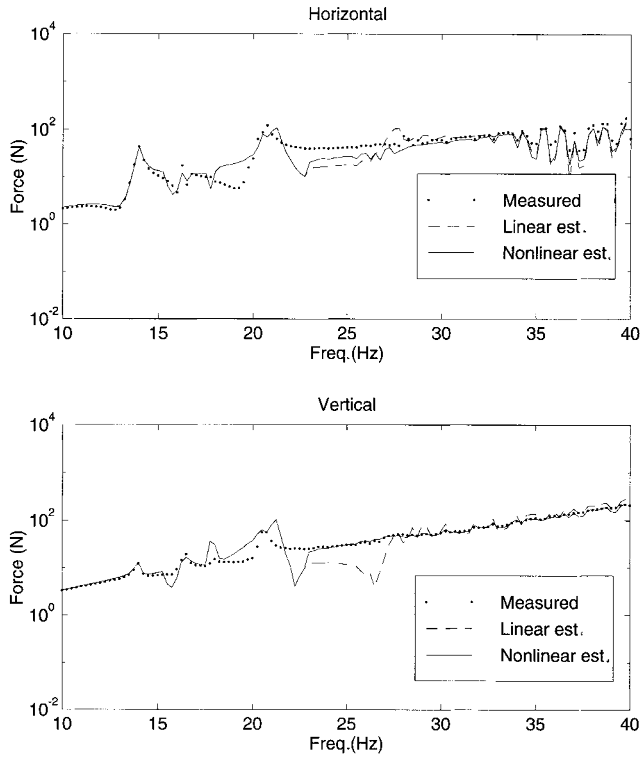

Fig. 7 Simulated and calculated forces with different excitation for bearing 1

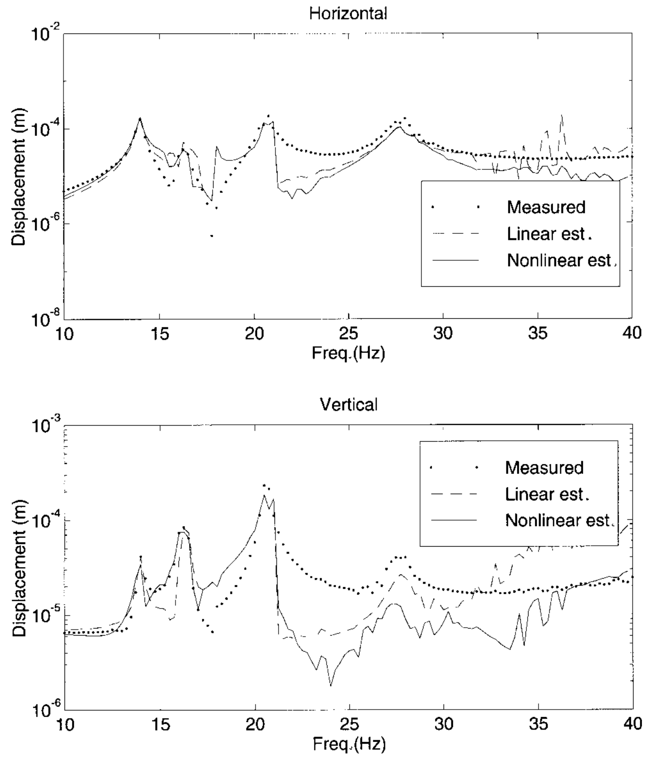

Fig. 9 Simulated and calculated displacements with different excitation for bearing 1

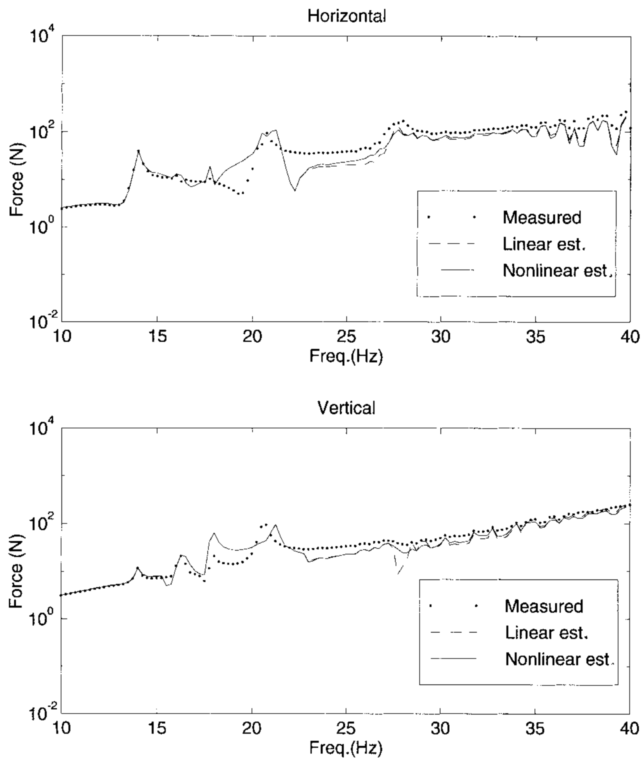

Fig. 8 Simulated and calculated forces with different excitation for bearing 2

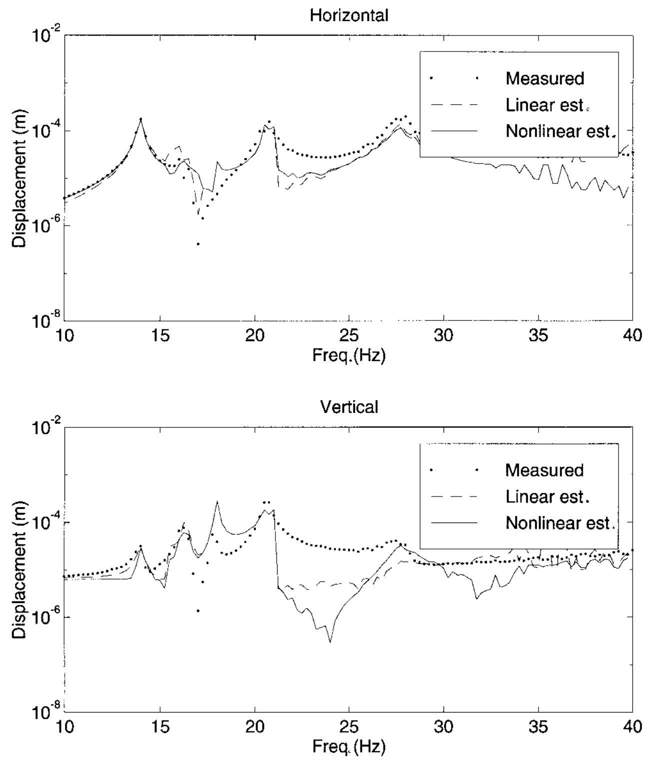

Fig. 10 Simulated and calculated displacements with different excitation for bearing 2

4 EXPERIMENTAL RESULTS

The method was then tested experimentally on the rig described above. Firstly, hammer tests were performed on the foundation without the rotor to obtain estimates of the natural frequencies and damping factors. Then the rotor was replaced and the machine run down from 40 Hz to rest to obtain responses due to the unbalance.

4.1 Impact tests

Impact tests were performed on the rotor shaft using a Brüel and Kjaer type 4370 accelerometer, PCB impact hammer and a Brüel and Kjaer type 2034 analyser. The FRFs were curve-fitted using the Star modal analysis package [23]. The shaft was suspended by elastic cords to simulate free–free boundary conditions. The theoretical and experimental frequencies are given in Table 4. Clearly there is very good agreement between the two.

Impact tests were also performed on the foundation pedestals, with the rotor removed but with the bearing housings in place. This yielded estimates of the foundation natural frequencies, which could be used later for verification of the estimated foundation model. Six frequencies were identified in the frequency range from 0 to 200 Hz and are shown in Table 5.

4.2 Run-down

The rotor was then ramped down in a linear fashion from 40 to 5 Hz over 6.5 min. The vibration was measured using four Bruël and Kjaer type 4370 accelerometers mounted in horizontal and vertical directions at each bearing. Data were acquired using a 16-channel analogue-to-digital converter. No anti-aliasing filters were used and vibration data from the accelerometers were sampled at 1000 Hz and from the keyphasor at 5000 Hz and then stored. A sinewave was fitted in a least-squares sense to the signal over 64 cycles, using the keyphasor signal as reference. This gave the magnitude and phase of the first synchronous component of the signal.

Three successive run-downs were performed, each with a different unbalance configuration. Firstly, a run-down was performed with no unbalance bolts attached to the balancing discs. Then two more run-downs were done with unbalance bolts placed as shown in Table 2. The displacement data from the second and third unbalance configurations were subtracted from those of the first to give the displacement due to the applied unbalance alone.

The acquired data from the run with the second unbalance configuration were used to calculate the forces on the bearings, from which the foundation parameters were estimated using both the linear and non-linear least-squares approaches. The frequency band width was split up into five ranges and a foundation model was estimated for each range. The ranges were then joined together to give the response for the total range.

Table 4 Rotor free–free frequencies obtained from hammer testing

Mode	Theory (Hz)	Experiment (Hz)	Error (%)
1	61.8	59.2	4.2
2	183.5	178.4	2.8
3	433.6	414.3	4.5
4	699.2	667.0	4.6

Table 5 Foundation pedestal frequencies from hammer testing

Mode	f (Hz)	ζ (%)
1	13.77	4.01
2	16.74	1.40
3	18.70	3.63
4	23.92	2.65
5	25.92	11.26
6	26.09	2.49

4.3 Results and discussion

Figures 11 to 18 show good fits between measurement and prediction for a given unbalance. Moreover, the non-linear output error estimates provide closer fits in general than the linear input error estimates.

However, the fits when testing the predictive capacity of the model excited by an unbalance different to that used for estimation were not quite as good, especially in the high-frequency range. One possible reason for this can be found by examining equation (2). It is obvious that the estimated forces and measured responses will both contain peaks at the global resonances of the entire machine. However, the data which are important for the foundation model will be found at the local foundation resonances, which may correspond to parts of the measured response with a low signal-to-noise ratio. This may also expand the results shown in Table 6, where in certain cases the frequencies of the identified foundation correspond to the global frequencies of the machine. A solution to this problem which is currently under investigation is estimating the foundation model in two steps:

(a) identifying the global modes of the machine,
(b) separating the foundation from this global model.

Secondly, there is the question of the uniqueness of the estimated model, which is essentially trying to map a measured set of outputs to a given set of inputs at each frequency. This mapping is not normally unique [**24**]. Traditional modal analysis helps enforce uniqueness by applying constraints to the transfer function matrix (like

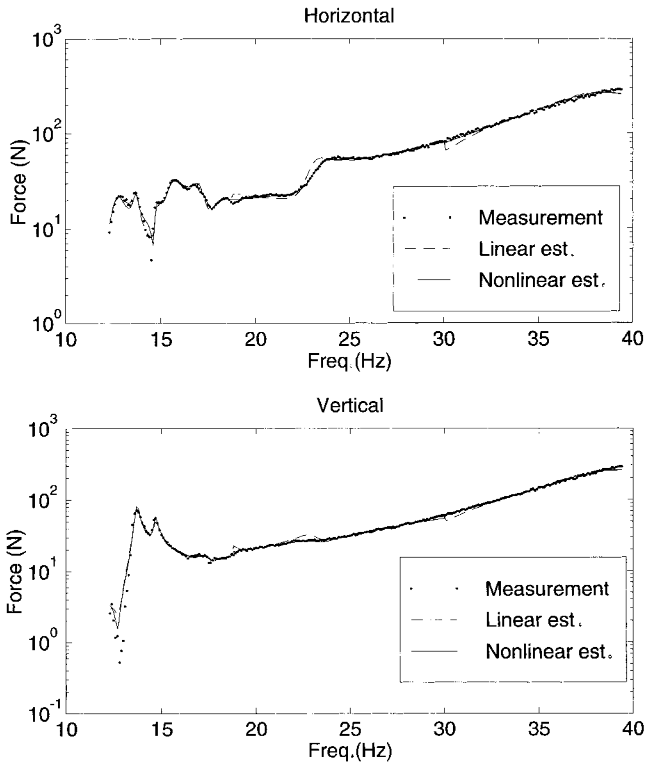

Fig. 11 Estimated and calculated forces for bearing 1

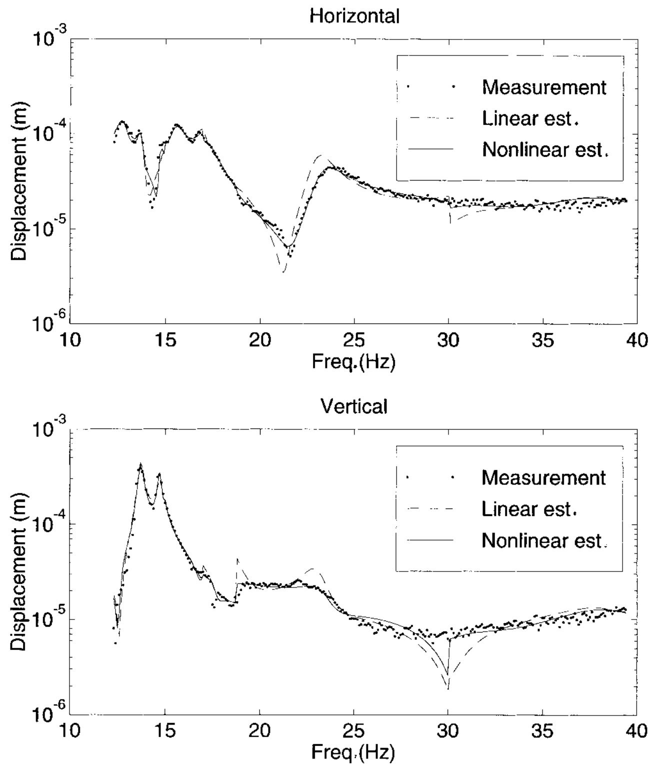

Fig. 13 Measured and calculated displacements for bearing 1

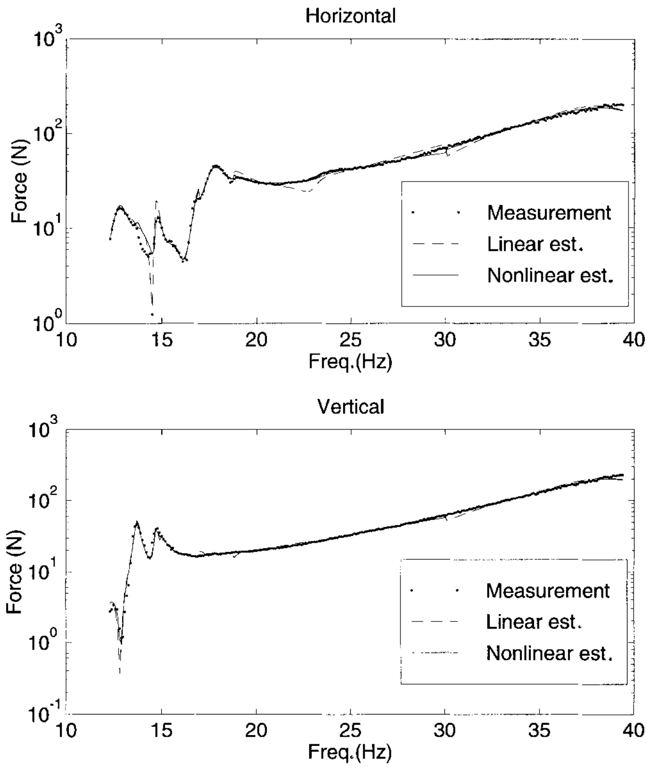

Fig. 12 Estimated and calculated forces for bearing 2

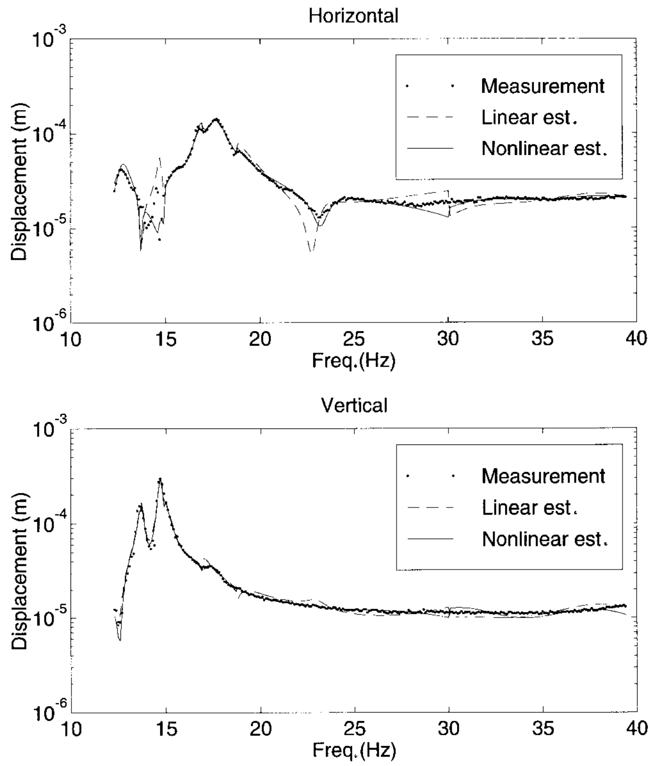

Fig. 14 Measured and calculated displacements for bearing 2

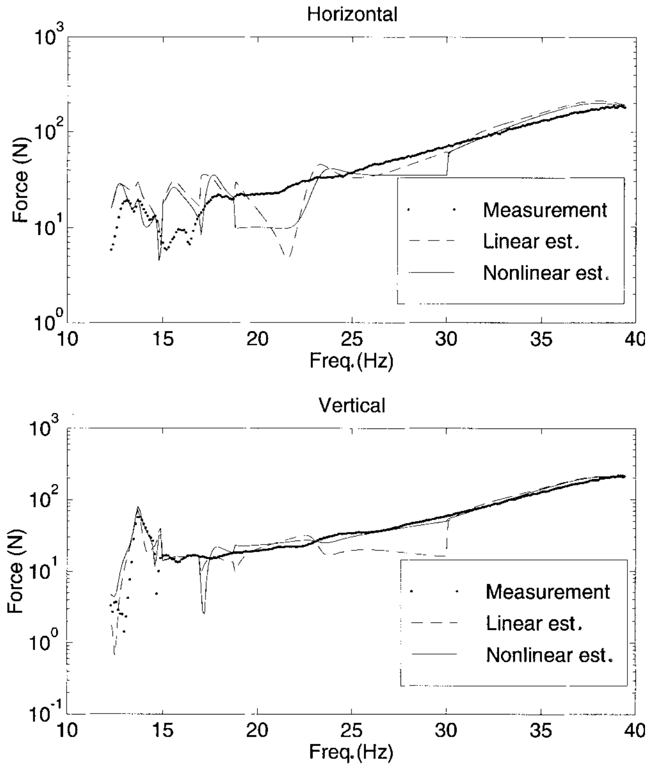

Fig. 15 Estimated and calculated forces with different excitation for bearing 1

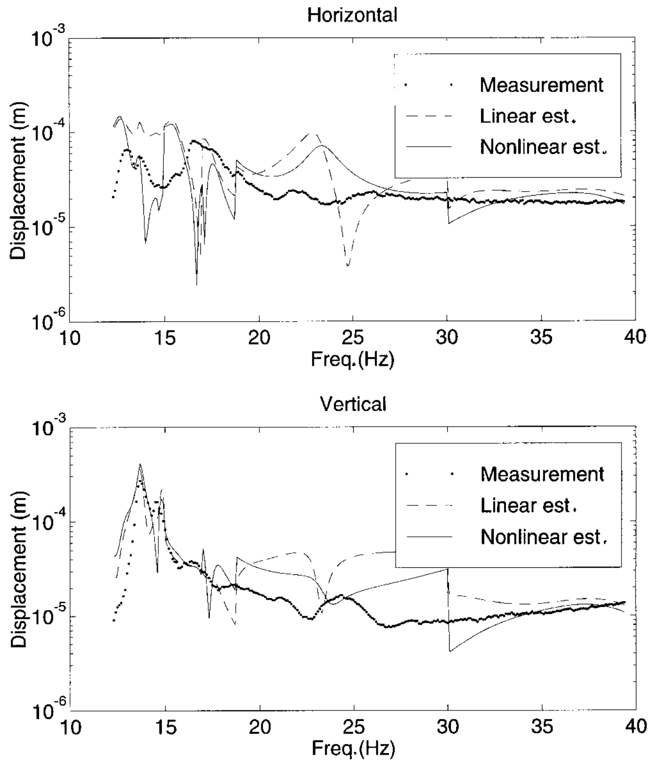

Fig. 17 Measured and calculated displacements with different excitation for bearing 1

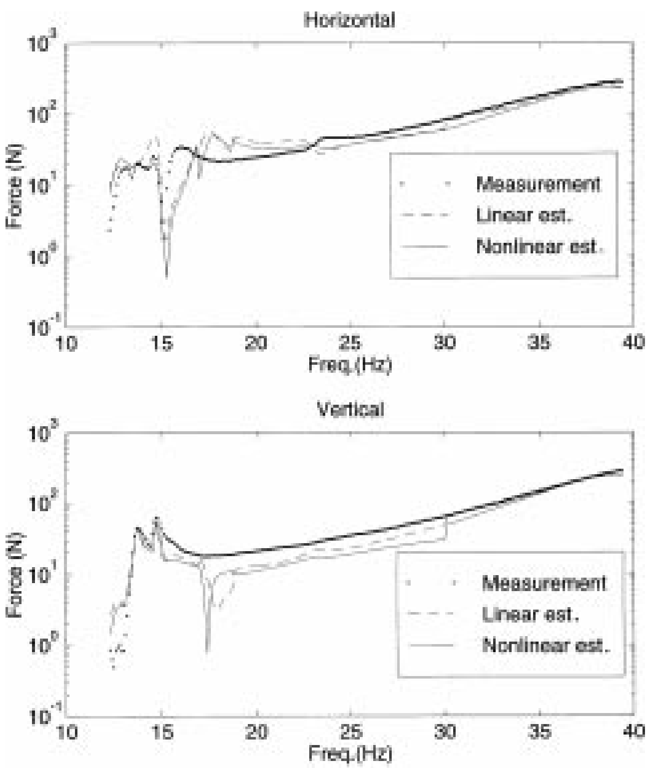

Fig. 16 Estimated and calculated forces with different excitation for bearing 2

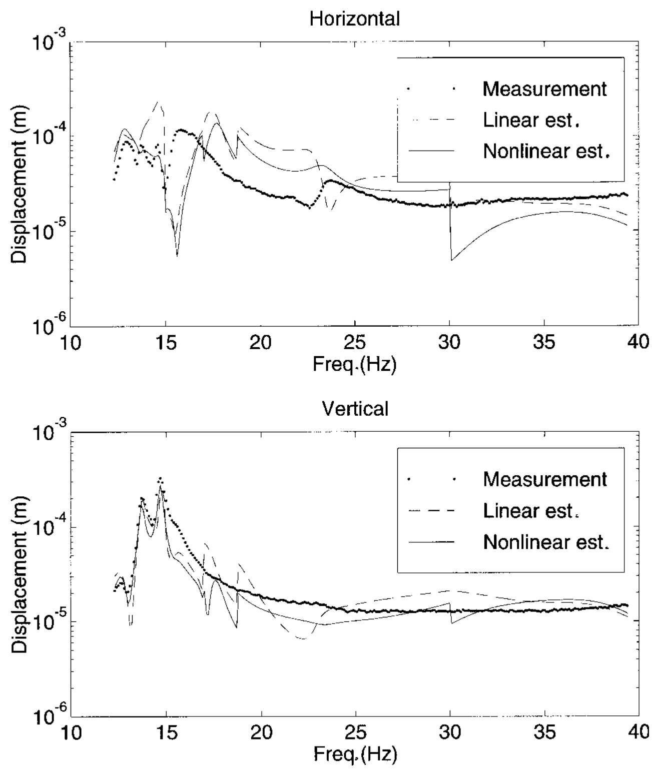

Fig. 18 Measured and calculated displacements with different excitation for bearing 2

Table 6 Estimated foundation frequencies and damping factors for experiment

Input error estimates		Output error estimates	
f (Hz)	ζ (%)	f (Hz)	ζ (%)
10.78	3.87	10.19	6.69
11.66	1.21	11.38	2.19
12.56	1.97	12.61	2.20
12.86	1.52	13.06	1.36
13.83	1.06	13.13	0.68
14.15	2.32	13.82	1.44
15.66	2.23	13.82	42.52
17.23	7.10	14.19	2.40
22.67	3.89	14.90	0.27
24.83	96.39	15.89	1.93
—	—	15.94	1.69
—	—	17.02	6.82
—	—	22.58	3.29
—	—	32.08	12.77

symmetry) and by parameterizing the transfer function in terms of modal parameters. Although this leads in general to a non-linear estimation problem, the resulting equations are not difficult to solve because each of the elements of the transfer function matrix are obtained independently. In the present case all directions are excited simultaneously and it is not possible to measure a displacement due to a single excitation. The question of the uniqueness of identified models is an important one in the literature (see, for example, reference [**7**]) and various types of regularization may be attempted [**25**].

Thirdly, the type of model being fitted (mass, damping and stiffness matrices) will only provide an exact fit if the foundation contains no internal DOF. This was clearly not the case and so the frequency range was split up to allow a better fit over each part. It is possible to use a more generalized frequency filter than equation (4) to take into account both numerator and denominator dynamics [**24**, **26**], but this approach can lead to other uniqueness problems since the estimated transfer function depends on the matrix polynomial powers.

Finally, the accuracy of the bearing model plays a part in the results. At certain frequencies the bearings can play a significant part in the overall dynamics of the machine and may therefore influence the accuracy of the forces which have been estimated. The bearing models used in this research must also be considered very approximate, since many factors such as temperature changes have been ignored and the static force used to calculate the coefficients may be seriously in error. Force transducers are currently being fitted to the test rig to measure the forces transmitted to the foundation. This will give some idea of the accuracy of the estimated forces.

5 CONCLUSIONS

A method for estimating turbogenerator foundation dynamic stiffness matrices from measured data obtained during run-down is presented and tested. By splitting the frequency range up into parts, good fits between measured and modelled displacements are obtained. However, the predictive capacity of the models when subjected to a different forcing function is more limited. Possible reasons for this situation are identified as poor signal-to-noise ratios at important frequency points, non-uniqueness of estimated parameters, the low-order models employed and incorrect bearing coefficients. Solving these problems is the subject of ongoing research.

6 ACKNOWLEDGEMENTS

The authors wish to acknowledge the support and funding of Nuclear Electric Limited and Magnox Electric plc. Dr Friswell gratefully acknowledges the support of the Engineering and Physical Sciences Research Council through the award of an Advanced Fellowship.

REFERENCES

1 **Lees, A. W.** and **Simpson, I. C.** The dynamics of turbo-alternator foundations. In Proceedings of IMechE Conference on *Steam and Gas Turbine Foundations and Shaft Alignment*, Bury St Edmunds, 1983, paper C6/83, pp. 37–44.

2 **Nichols, T.** and **Simpson, I. C.** A summary of tests carried out to determine the dynamic properties of Didcot unit 2 steel turbo-alternator foundations. Technical Report SWR/SSD/0238/N/83, CEGB, 1983.

3 **Lees, A. W.** The least squares method applied to identify rotor/foundation parameters. In Proceedings of IMechE International Conference on *Vibrations in Rotating Machinery*, Edinburgh, 1988, paper 306/88, pp. 209–216.

4 **Vania, A.** Identification of the modal parameters of rotating machine foundations. Technical Report, Dipartimento di Meccanica, Politecnico Di Milano, 1996.

5 **Feng, N. S.** and **Hahn, J.** Including foundation effects on the vibration behaviour of rotating machinery. *Mech. Systems and Signal Processing*, 1995, **9**(3), 243–256.

6 **Zanetta, G. A.** Identification methods in the dynamics of turbogenerator rotors. In Proceedings of IMechE International Conference on *Vibrations in Rotating Machinery*, Bath, 1992, paper 432/092, pp. 173–181.

7 **Van den Hof, P. M. J.** Model sets and parameterizations for identification of multivariate equation error models. *Automatica*, 1994, **30**(3), 433–446.

8 **Schoukens, J.** and **Pintelton, R.** *Identification of Linear Systems*, 1991 (Pergamon Press, Oxford).

9 **Mottershead, J. E.** and **Stanway, R.** Identification of structural vibration parameters by using a frequency domain filter. *J. Sound Vibr.*, 1986, **109**, 495–506.

10 **Mottershead, J. E., Lees, A. W.** and **Stanway, R.** A linear, frequency domain filter for parameter identification of vibrating structures. *J. Vibr. Acoust., Stress and Reliability in Des.*, 1987, **109**, 262–269.

11 **Mottershead, J. E.** A unified theory of recursive, frequency

domain filters with application to system identification in structural dynamics. *J. Vibr. Acoust., Stress and Reliability in Des.*, 1988, **110**, 360–365.

12 **Braun, S. G.** and **Ram, Y. M.** Structural parameter identification in the frequency domain: the use of overdetermined systems. *J. Dynamic Systems, Measmt and Control*, 1987, **109**, 120–123.

13 **Braun, S.** and **Ram, Y.** Time and frequency identification methods in over-determined systems. *Mech. Systems and Signal Processing*, 1987, **1**(3), 245–257.

14 **Friswell, M. I., Lees, A. W., Smart, M. G.** and **Prells, U. P.** Identifying noise modes in estimated turbogenerator foundation models. In Proceedings of Conference on *Modern Practice in Stress and Vibration*, Dublin, 1997, pp. 57–64 (Institute of Physics).

15 **Natke, H. G., Lallemant, G., Cottin, N.** and **Prells, U.** Properties of various residuals within updating of mathematical models. In *Inverse Problems in Engineering*, Vol. 1, 1995, pp. 329–348 (Overseas Publishers Association, Amsterdam).

16 **Smart, M. G., Friswell, M. I., Lees, A. W.** and **Prells, U.** Errors in estimating turbo-generator foundation parameters. In Proceedings of ISMA 21, Katholieke Universiteit, Leuven, Belgium, 1996, pp. 1225–1235.

17 **Fritzen, C. P.** Identification of mass, damping and stiffness matrices of mechanical systems. *J. Vibr., Acoustics, Stress and Reliability in Des.*, 1986, **108**, 9–17.

18 **Golub, G. H.** and **Van Loan, C. F.** *Matrix Computations*, 1990 (John Hopkins, Baltimore, Maryland).

19 **Moré, J. J.** and **Wright, S. J.** *Optimization Software Guide*, 1993 (SIAM, Philadelphia, Pennsylvania).

20 **Gill, P. E., Murray, W.** and **Wright, M. H.** *Practical Optimization*, 1981 (Academic Press, New York).

21 **Smith, D. M.** *Journal Bearings in Turbomachinery*, 1969 (Chapman and Hall, London).

22 **Hisa, S.** and **Matsuura, T.** Experiments on the dynamic characteristics of large scale journal bearings. In Proceedings of 2nd IMechE International Conference on *Vibrations in Rotating Machinery*, Cambridge, 1988, paper C284/80, pp. 223–230.

23 *Star System User's Guide*, 1994 (General Structural Test Products).

24 **Jain, V. K.** and **Sarkar, T. K.** Multivariable system identification by pencil-of-functions method. *IEEE Trans. Instrumn and Measmt*, 1985, **34**(4), 550–557.

25 **Natke, H. G., Cottin, N.** and **Prells, U.** Problems and related countermeasures in mathematical model improvement: a survey. In Proceedings of ICOSSAR 93: The 6th International Conference on *Structural Safety and Reliability* (Eds G. Schuller, M. Shinozuka and J. Yao), Rotterdam, 1994, pp. 821–827 (Balkema).

26 **Van Der Auweraer, H.** and **Leuridan, J.** Multiple input orthogonal polynomial parameter estimation. *Mech. Systems and Signal Processing*, 1987, **1**(3), 259–272.